Metastable lattice of droplets in phase separating polymer blends

Sergey Panyukov and Yitzhak Rabin
Department of Physics, Bar-Ilan University, Ramat-Gan 52900, Israel
(Received 7 February 2002; published 21 June 2002)

Phase separation in a polymer mixture with an off-critical composition is described by a Ginzburg-Landau Hamiltonian that contains both cubic and quartic terms in the deviation of composition from its mean value in the homogeneous phase. Our analysis suggests that when a blend is brought in the vicinity of the spinodal, the initial homogeneous phase becomes unstable against the formation of a metastable lattice of spherical droplets whose lifetime diverges in the limit of infinite molecular weight. The composition of the droplets approaches that of the background phase and their size diverges with the approach to the critical point, but the composition contrast is enhanced and droplet radii become comparable to polymer dimensions, away from criticality. The connection between our predictions and the results of recent neutron scattering experiments is discussed, and new experiments that could probe the proposed droplet lattice are proposed.

DOI: 10.1103/PhysRevE.65.061803 PACS number(s): 64.60.Qb, 61.41.+e, 83.80.Tc

I. INTRODUCTION

The study of phase separation in polymer blends is important for elucidating the fundamental limitations on the practically important task of mixing different polymers in order to obtain composites with tunable material properties. It is usually thought that the physical mechanisms governing incompatibility and segregation in polymer blends are quite similar to those in mixtures of small molecules and that the differences between the two cases are mainly quantitative and can be summarized as follows.

(1) Because high molecular weight reduces the entropy of mixing, the region of the phase diagram in which two polymers can be mixed in all proportions is strongly reduced compared to that of their monomeric counterparts.

(2) Since each polymer is permeated by many others, the fluctuations of relative concentration of the two components in the mixture are suppressed and mean field approximations have a much larger domain of applicability than in mixtures of small molecules [1].

An indication that something peculiar takes place in polymer blends came from light scattering studies of phase separation following a temperature quench at an off-critical composition [2,3]. Initially, the peak of the scattered intensity moved with time to progressively longer wavelengths, exhibiting the coarsening of the demixing pattern characteristic of spinodal decomposition [4]. However, at later times it became pinned at some wavelength whose value depended on the location of the quench and on the molecular weight of the constituents, and no further change with time was observed [2]. Direct visualization by computer-enhanced microscopy showed an arrested pattern that consisted of nearly spherical droplets of roughly equal size [3] (in this particular experiment, the droplets eventually coalesced and phase separation continued following a long incubation period). Attempts to explain the observed pinning invoked slowing down of polymer diffusion due to entropic barrier created for the transport of long chains across sharp interfaces between phase-separated domains [5], and preferential interaction of the bounding surfaces with one of the components in a quasi-two-dimensional polymer film [6].

Motivated by these observations, in this paper we reexamine the nature of metastability in polymer blends. Our analysis shows that when a blend with an off-critical composition is quenched into the vicinity of the spinodal, the classical nucleation scenario breaks down and the initial homogeneous phase becomes unstable with respect to the formation of droplets with size comparable to polymer dimensions, and with composition that differs from that of the equilibrium daughter phase. In Sec. II we introduce the standard de Gennes–Flory–Huggins free energy of an asymmetric polymer blend, which accounts for entropy of mixing, interaction, and entropic elasticity of polymer chains [7], and upon some transformations derive the Ginzburg-Landau (GL) Hamiltonian that describes the energy cost of deviations from the homogeneous state. We analyze the thermodynamics of phase separation, review the main results of the classical theory of nucleation for shallow quenches into the metastable region in vicinity of the binodal, and discuss the anticipated breakdown of this theory for deeper quenches. In Sec. III we show that the cubic term in the GL Hamiltonian can be replaced by a position-dependent fluctuating temperature field and rewrite the free energy of the blend in a form familiar from the theory of superconductivity in a random field. This random field acts as an effective potential well that leads to the appearance of a localized spherical droplet solutions. The single droplet free energy is expressed as the sum of droplet energy and density of states contributions (logarithmic corrections due to Goldstone modes are derived in Appendix A). Using the ground state dominance approximation we derive an explicit solution for the droplet profile and its energy (an exact solution obtained by numerical minimization of the energy functional is presented in Appendix B). We show that in the vicinity of the spinodal, the distribution function of isolated droplets has a sharp peak at a well-defined droplet radius that is bounded below by the polymer radius of gyration and diverges as the critical composition is approached. Since the depth of the corresponding minimum of the free energy diverges with the square root of the degree of polymerization, we conclude that (a) droplet

solutions correspond to long-lived metastable states of the blend, and that (b) droplets will appear spontaneously everywhere in the system upon quench into the vicinity of the spinodal. In order to gain insight about the many-droplet solution, in Sec. IV we analyze the interaction between two isolated droplets. At large separations, the interaction is of repulsive Yukawa type, with screening radius given by the correlation length, and thus droplets are expected to form until the free energy gain due to their self-energy is balanced by interdroplet repulsions. Variational minimization of the many-droplet free energy shows that the ''lattice of droplets'' picture is self-consistent in the sense that the interdroplet spacing is much larger than their radius and that the interaction between droplets has only a minor effect on their internal concentration profile (at least in the vicinity of the spinodal). Finally, in Sec. V we summarize the main results of this work and discuss the limitations of our approach. The connection between our results and available neutron scattering data is discussed and new experiments that could test our ideas are proposed.

II. PHASE SEPARATION: THERMODYNAMICS AND NUCLEATION

Consider a two-component polymer blend where N and θN are the respective numbers of statistical segments per chain (θ is the asymmetry parameter; $\theta=1$ for a symmetric blend) and a is a microscopic length scale, of the order of the statistical segment length (for simplicity, we use a single length scale to represent both the Kuhn length and the size of the lattice site). The effective ''Hamiltonian'' of the blend is the de Gennes–Flory–Huggins free energy that can be written as a functional of the volume fractions of the two components $\phi_1=\phi$ and $\phi_2=1-\phi$, respectively [7],

$$\frac{H}{k_BT}=\int\frac{d\mathbf{x}}{a^3}\left[\frac{a^2}{8}\frac{(\nabla\phi)^2}{\phi(1-\phi)}+U(\phi)-\mu\phi\right], \tag{1}$$

where k_B is the Boltzmann constant and T is the temperature, and the integration extends over the volume of the blend. The potential $U(\phi)$ is given by the Flory-Huggins expression for the free energy per site [8]

$$U(\phi)=\frac{\phi}{N}\ln\phi+\frac{1-\phi}{\theta N}\ln(1-\phi)+\chi\phi(1-\phi), \tag{2}$$

where the Flory interaction parameter $\chi(T)$ is, in general, a function of the temperature T. The chemical potential of component 1, is defined by $\mu=dU/d\phi|_{\phi=\bar{\phi}}$, and thus,

$$\mu=\frac{1}{N}\ln\bar{\phi}+\frac{1}{N}-\frac{1}{\theta N}\ln(1-\bar{\phi})-\frac{1}{\theta N}-2\chi\bar{\phi}+\chi, \tag{3}$$

where $\bar{\phi}$ is the mean volume fraction of component 1. Inspection of Eq. (2) shows that, for $\chi<0$, the entropy of mixing dominates over the effective repulsive interaction between the two components and they are miscible in all proportions. For positive and sufficiently large values of χ, repulsion dominates and demixing of the two components takes place in equilibrium. The coexistence line (binodal) in the χ-ϕ plane that describes the volume fractions of component 1 in the two coexisting phases in equilibrium is found by minimizing the function

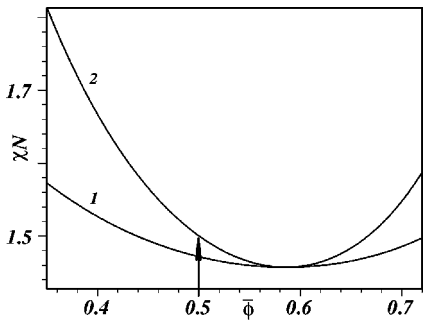

FIG. 1. Phase diagram for $\theta=0.5$, $\bar{\phi}=0.5$. The binodal (1) and spinodal (2) lines are shown. The arrow indicates the position on the phase diagram into which the system is quenched.

$$N\chi(\phi,\phi')=\frac{1}{\phi-\phi'}\left(1-\frac{1}{\theta}\right)+\frac{1}{(\phi-\phi')^2}\times\left(\phi'\ln\frac{\phi'}{\phi}+\frac{1-\phi'}{\theta}\ln\frac{1-\phi'}{1-\phi}\right) \tag{4}$$

with respect to ϕ'. The value of the Flory parameter at the binodal, $\chi_{bin}=\chi[\bar{\phi},\phi'_{\min}(\bar{\phi})]$, is obtained by substituting the resulting $\phi'_{\min}$ (the volume fraction in the phase that coexists with a phase of volume fraction $\phi=\bar{\phi}$) back into Eq. (4) (see Fig. 1).

In order to transform the square gradient term in Eq. (1) into the standard GL expression, we substitute $\phi=\sin^2\varphi$, where $0<\varphi<\pi/2$ and get

$$\frac{H}{k_BT}=\int\frac{d\mathbf{x}}{a^3}\left[\frac{a^2}{2}(\nabla\varphi)^2+U(\sin^2\varphi)-\mu\sin^2\varphi\right]. \tag{5}$$

Expanding φ about its mean value,

$$\varphi=\arcsin\sqrt{\bar{\phi}}+a^{3/2}\psi \tag{6}$$

we can write the Hamiltonian as $H=H_0(\bar{\phi})+\Delta H[\psi]$ where

$$\frac{H_0(\bar{\phi})}{k_BT}=\frac{V}{a^3}[U(\bar{\phi})-\mu\bar{\phi}], \tag{7}$$

with V the volume of the blend. The Hamiltonian ΔH that describes the deviations from the homogeneous solution has the GL form

$$\frac{\Delta H[\psi]}{k_BT}=\int d\mathbf{x}\left[\frac{a^2}{2}(\nabla\psi)^2+\frac{\tau}{2}\psi^2-\frac{g_3}{6}\psi^3+\frac{g_4}{24}\psi^4\right]. \tag{8}$$

The coefficients of the expansion (to fourth order in ψ) in the above expression are

$$\tau=\frac{4}{N}[1-\bar{\phi}+\theta\bar{\phi}-2\chi N\bar{\phi}(1-\bar{\phi})],$$

$$g_3=\frac{8a^{3/2}}{N\sqrt{\bar{\phi}(1-\bar{\phi})}}[(1-\bar{\phi})^2-\theta\bar{\phi}^2], \tag{9}$$

$$g_4=\frac{16a^3}{N\bar{\phi}(1-\bar{\phi})}[(1-\bar{\phi})^2(4\bar{\phi}-1)+\theta\bar{\phi}^2(3-\overline{4\phi})].$$

The above expansion is valid for $g_4>0$. For $\theta=0.5$ this condition holds in the range $0.23<\bar{\phi}<0.81$.

The mean field spinodal (the boundary of stability of the spatially homogeneous state of the blend) is defined by the condition $\tau=0$, or equivalently by

$$\chi_{sp}N=\frac{1}{2\bar{\phi}}+\frac{\theta}{2(1-\bar{\phi})}. \tag{10}$$

The binodal and the spinodal coincide at the critical point defined by $g_3=0$ (Fig. 1). This yields the critical volume fraction

$$\bar{\phi}_c=\frac{1}{1+\sqrt{\theta}}. \tag{11}$$

Consistent with the fact that the Landau expansion holds only in the vicinity of the critical point, we substituted $\chi=\chi_{sp}$ in the expressions for the coefficients g_3 and g_4 that will be treated as temperature-independent parameters in the following [the remaining temperature dependence is due to the fact that τ is a function of $\chi(T)$, Eq. (9)]. In general, fluctuations shift the spinodal of the spatially homogeneous system to some finite $\tau\simeq\tau_G$ where the Ginzburg number τ_G defines the boundary of applicability of the mean field theory (the Ginzburg region). However, it can be shown [7,9] that $\tau_G\to 0$ in the limit $N\to\infty$ and therefore, in polymer systems, the mean field approximation is expected to yield accurate results even in the vicinity of the spinodal.

The fluctuational contribution to the total free energy of the blend is given by

$$\Delta F=-k_BT\ln\int D\psi\exp\left(-\frac{\Delta H[\psi]}{k_BT}\right). \tag{12}$$

Inspection of Eq. (6) shows that the field ψ is related to the deviation of the volume fraction of component 1 from its mean value,

$$\delta\phi=2a^{3/2}\sqrt{\bar{\phi}(1-\bar{\phi})}\,\psi. \tag{13}$$

In addition to small fluctuations about the homogeneous state in the one-phase region of the phase diagram, the GL Hamiltonian governs the kinetics of phase separation and the formation of macroscopic density inhomogeneities following a quench into the two-phase region, $\chi>\chi_{bin}$. According to the common view, segregation takes place via nucleation and growth or via spinodal decomposition, depending on whether the system is quenched into a metastable or an unstable region of the phase diagram. In the latter case, the initial homogeneous phase decays via small amplitude, delocalized fluctuations whose amplitude and wavelength grow with time until final phase separation is reached. For quenches into the metastable region, the initially homogeneous state decays by the formation of large amplitude, localized fluctuations that correspond to a saddle point of $\Delta H[\psi]$, Eq. (8). Near the binodal $\tau=\tau_b(\bar{\phi})=g_3^2/(3g_4)$, this saddle point (critical nucleus) configuration of the field ψ is given by

$$\psi_{cn}(r)=\frac{\psi'}{\exp[(r-R_c)/\xi]+1}, \tag{14}$$

where r is the radial coordinate and we defined $R_c=(a\tau_b^{1/2}/3)(\tau_b-\tau)^{-1}$, $\xi=a\tau_b^{-1/2}$, and $\psi'=2g_3/g_4$. Inspection of Eq. (14) shows that this configuration describes a spherically symmetric nucleus with a large core of radius R_c and nearly constant volume fraction ϕ' that coincides with that of the new (daughter) phase, and a narrow interface of width ξ in which this density changes to that of the mother phase (in the vicinity of the binodal, $R_c\gg\xi$). Notice that this solution corresponds to a saddle point of the GL Hamiltonian in the sense that while nonspherical nuclei have a higher energy than spherical ones, a nucleus of critical size has the highest energy among all spherical nuclei with radii either smaller or larger than R_c. In order to reach the thermodynamically favored macroscopic daughter phase, any small nucleus created in the process of thermal fluctuations from the initial homogeneous mother phase has to pass through the energy barrier associated with the critical configuration (nuclei with $R>R_c$ grow without limit). This energy barrier is given by,

$$\Delta H[\psi_{cn}]=\frac{4\pi}{81}\frac{g_3^2}{g_4^2\tau_b^{1/2}(1-\tau/\tau_b)^2}\sim\frac{|\bar{\phi}-\bar{\phi}_c|N^{1/2}}{(1-\tau/\tau_b)^2}. \tag{15}$$

Since the probability of formation (in the process of thermal fluctuations) of the critical nucleus from the initial homogeneous phase is proportional to $\exp\{-\Delta H[\psi_{cn}]/k_BT\}$, the fact that the height of the barrier diverges at the binodal means that the initial homogeneous phase is metastable under shallow quenches beyond the binodal, and that critical nuclei will form on experimentally accessible time scales only for sufficiently deep quenches. In low molecular weight mixtures ($N\simeq 1$), one reaches the so called cloud point at which critical nuclei form and grow throughout the system immediately following the quench. This happens at some finite value of $1-\tau/\tau_b$, when the height of the barrier becomes comparable to k_BT, and at the same time $R_c\simeq\xi$ (for small molecules, away from the critical point, the correlation length approaches their microscopic dimension a), signaling the breakdown of the critical nucleus solution, Eq. (14). The cloud point defines the experimentally observable limit of metastability and is often considered as an operational definition of the spinodal. This can be understood theoretically if we notice that in mixtures of small molecules the Ginzburg

number is large and the mean field spinodal is shifted considerably towards the metastable region.

A different situation arises in polymer blends in which the correlation length is large even away from criticality, $\xi \sim aN^{1/2}$. In this case the critical nucleus scenario also breaks down at some finite value of $1-\tau/\tau_b$, when the size of the nucleus becomes of the order of its interfacial width ($R_c \simeq \xi$). Since, at this point the height of the energy barrier is of order $k_BTN^{1/2} \gg k_BT$, it does not represent the limit of metastability and the onset of spinodal decomposition is preempted by the appearance of a new metastable phase. This is a consequence of the fact that since the Ginzburg number vanishes in the limit of large N, the mean field spinodal is not shifted by fluctuations and therefore the phase diagram contains a finite region (somewhere in the vicinity of line 2 in Fig. 1) in which critical nuclei are no longer formed but the system is still stable against small amplitude, long wavelength fluctuations. This metastable phase corresponds to a true local minimum of $\Delta H[\psi]$ and consists of a lattice of droplets of well defined size whose composition differs from that of the final equilibrium phase and varies continuously with the distance from the center of the droplet.

III. SINGLE DROPLET SOLUTION

In the following we show that there is a range of parameters in which the partition function of a system described by the Hamiltonian, Eq. (8), is dominated by stable droplet configurations (instantons [10]). In our analysis we will use the analogy between our problem and superconductivity in a random field [11] where droplets of the superconducting phase form in a sample with quenched spatial distribution of transition temperatures. Notice that both models reduce to the ψ^4 theory of second order phase transitions if one switches off the cubic (in ψ) term in our Hamiltonian and the random field in Ref. [11]. In order to transform our theory to the form of Ref. [11], we get rid of the cubic term in the Hamiltonian, Eq. (8), by introducing an auxiliary field, $\eta(\mathbf{x})$ ($\eta \geqslant 0$), through the functional integral,

$$\left\langle \exp\left(\frac{1}{2}\int d\mathbf{x}\,\eta\psi^2\right)\right\rangle_\eta \simeq \exp\left[\frac{g_3}{6}\int d\mathbf{x}\psi^3\right], \tag{16}$$

where we defined the functional average of an arbitrary functional $A[\eta]$,

$$\langle A\rangle_\eta = \frac{\int D\eta \exp(-S[\eta])A[\eta]}{\int D\eta \exp(-S[\eta])}, \tag{17}$$

with

$$S[\eta] = \frac{2}{3g_3^2}\int d\mathbf{x}\,\eta^3(\mathbf{x}). \tag{18}$$

The approximate equality, Eq. (16), holds if the functional integral is evaluated by steepest descent (this procedure is valid for $S[\eta_{\min}] \gg 1$, where $\eta_{\min}(\mathbf{x})$ is the function that minimizes $S[\eta]$).

We now substitute Eq. (16) into Eqs. (8) and (12), and find

$$\Delta F = -k_BT \ln\left\langle \int D\psi \exp\left(-\frac{H_\eta[\psi]}{k_BT}\right)\right\rangle_\eta, \tag{19}$$

where $H_\eta[\psi]$ is the effective Hamiltonian of a ψ^4-type theory in an external field η,

$$\frac{H_\eta[\psi]}{k_BT} = \int d\mathbf{x}\left[\frac{\tau-\eta}{2}\psi^2 + \frac{a^2}{2}(\nabla\psi)^2 + \frac{g_4}{24}\psi^4\right]. \tag{20}$$

This completes our demonstration of the connection between our theory and that of superconductivity in a random field. The analogy extends even further since in both problems the Ginzburg number is vanishingly small due to the existence of large intrinsic length scales (the polymer radius $aN^{1/2}$ in blends and the correlation length of Cooper pairs in superconductivity). However, even though the Hamiltonian in Eq. (20) is identical to that in Ref. [11], the free energies differ since in our case one carries out a thermal average of the partition function over the random field η, while in Ref. [11] the random field is quenched and therefore one averages the logarithm of the partition function. We show in the following that the typical configuration of the field $-\eta(\mathbf{x})$ corresponds to a spatial distribution of potential wells of sufficient depth, and that the field $\psi(\mathbf{x})$ is localized in these potential wells. Consequently, the density field can be described as a collection of droplets.

Consider a single droplet configuration $\psi(\mathbf{x})$ localized in a potential well, $-\eta_{drop}(\mathbf{x})$ around $\mathbf{x}=0$. Following Ref. [11] we assume that (a) one can treat the problem perturbatively (for small g_4) by expanding the solution in eigenfunctions of the linear problem defined by the quadratic part of the Hamiltonian, Eq. (20) and that (b) one can keep only the ground state contribution to this expansion. This allows one to write a variational solution in the form

$$\psi(\mathbf{x}) = c_0\psi_0(\mathbf{x}), \tag{21}$$

where $\psi_0(\mathbf{x})$ is an eigenfunction of the Schrödinger equation that corresponds to the smallest eigenvalue λ_0 of the Schrödinger operator $\tau - \eta_{drop} - a^2\nabla^2$ (the kernel of the quadratic part of $H_\eta[\psi]$),

$$(\tau - \eta_{drop} - a^2\nabla^2)\psi_0 = \lambda_0\psi_0. \tag{22}$$

As usual, the eigenfunction is normalized as

$$\int d\mathbf{x}\psi_0^2(\mathbf{x}) = 1. \tag{23}$$

Substituting $\psi = c_0\psi_0$ into the Hamiltonian, Eq. (20), and minimizing the resulting expression with respect to the amplitude c_0 yields,

$$c_0^2 = -\frac{6\lambda_0}{g_4}\left(\int d\mathbf{x}\psi_0^4\right)^{-1}. \tag{24}$$

Clearly, a solution exists only for $\lambda_0 < 0$. Inserting this expression into Eq. (20), we obtain a variational estimate for the energy of a droplet

$$\frac{E^0_{drop}(\lambda_0)}{k_B T} = -\frac{3}{2}\frac{\lambda_0^2}{g_4}\left(\int d\mathbf{x}\psi_0^4\right)^{-1}. \tag{25}$$

The single droplet contribution to the partition function [the expression in the brackets in Eq. (19)] can be written as

$$\int D\psi \exp\left(-\frac{H_\eta[\psi]}{k_B T}\right) \simeq \exp\left[-\frac{E_{drop}(\lambda_0)}{k_B T}\right], \tag{26}$$

where the energy of the droplet in a given energy well η_{drop} is

$$\frac{E_{drop}(\lambda_0)}{k_B T} = \min_{\psi}\frac{H_\eta[\psi]}{k_B T}. \tag{27}$$

Substituting Eq. (26) and the left-hand side of the equality

$$\int d\lambda\, \delta(\lambda - \lambda_0[\eta]) = 1 \tag{28}$$

into the integrand of Eq. (19), we find the free energy of a droplet,

$$\Delta F_{drop} = -k_B T \ln\left\{\int_{-\infty}^{0} d\lambda g(\lambda)\exp\left[-\frac{E_{drop}(\lambda)}{k_B T}\right]\right\}, \tag{29}$$

where the density of states $g(\lambda)$ is defined as

$$g(\lambda) = \langle \delta[\lambda - \lambda_0(\eta)]\rangle_\eta. \tag{30}$$

We proceed to calculate the density of states by steepest descent evaluation of the functional integral that defines the above average [Eq. (17)]. Minimizing $S[\eta]$, Eq. (18), and taking into account the condition $\lambda_0(\eta) = \lambda$, by introducing a Lagrange multiplier α, we find the following equation for the single droplet potential well $\eta_{drop}(\mathbf{x})$,

$$\frac{2}{g_3^2}\eta_{drop}^2 + \alpha\frac{\delta\lambda_0[\eta_{drop}]}{\delta\eta_{drop}} = 0. \tag{31}$$

The variational derivative $\delta\lambda_0/\delta\eta$ can be calculated from the variational principle for the lowest eigenvalue of the quadratic contribution to $H_\eta[\psi]$, Eq. (20),

$$\lambda_0[\eta] = \min_{\psi_0}\int d\mathbf{x}[(\tau - \eta)\psi_0^2 + a^2(\nabla\psi_0)^2]. \tag{32}$$

Taking the functional derivative of both sides of this equation with respect to $\eta(\mathbf{x})$ gives

$$\frac{\delta\lambda_0[\eta]}{\delta\eta(\mathbf{x})} = -\psi_0^2(\mathbf{x}). \tag{33}$$

Substituting Eq. (33) into Eq. (31) we arrive at the expression

$$\eta_{drop}(\mathbf{x}) = \sqrt{\alpha/2}\, g_3 \psi_0(\mathbf{x}) \tag{34}$$

Inserting Eq. (34) into Eq. (22) with $\varepsilon_0 = \varepsilon$, we find the self-consistent equation for the function $\psi_0(\mathbf{x})$,

$$(\tau - \sqrt{\alpha/2}\, g_3\psi_0 - a^2\nabla^2)\psi_0 = \lambda\psi_0. \tag{35}$$

Clearly, the eigenfunction ψ_0 corresponding to the lowest eigenvalue is spherically symmetric and depends only on the radial coordinate, r. The Lagrange multiplier α is found from the normalization condition, Eq. (23). It is convenient to introduce the dimensionless distance $t = r\sqrt{\tau - \lambda}/a$, and define the dimensionless function $\chi(t)$ by

$$\psi_0(r) = \sqrt{\frac{2}{\alpha}}\frac{\tau - \lambda}{g_3}\chi\left(\frac{r\sqrt{\tau - \lambda}}{a}\right). \tag{36}$$

With these substitutions, Eq. (35) is recast into the dimensionless form,

$$\chi'' + 2\chi'/t = \chi - \chi^2, \tag{37}$$

where prime denotes differentiation with respect to t. This equation is solved subject to the boundary conditions

$$\chi(t\to\infty) = 0,\ \ \chi'(0) = 0, \tag{38}$$

where the first condition corresponds to a localized droplet state and the second one ensures that $\chi(0)$ is finite. The above equation is solved by numerical integration of Eq. (37). The asymptotic form of this solution at $t \gg 1$ is

$$\chi(t) \approx t^{-1}e^{-t}. \tag{39}$$

At small $t \ll 1$ the solution is given by the series expansion

$$\chi(t) = \chi(0)\left[1 - \frac{\chi(0) - 1}{6}t^2 + \cdots\right]. \tag{40}$$

Equations (36) and (39) show that the characteristic dimension of the droplet is $t \simeq 1$. Reinstating dimensional units, the droplet size is expressed through the parameter λ as

$$R(\lambda) = \frac{a}{\sqrt{\tau - \lambda}}. \tag{41}$$

Substituting Eq. (36) into the normalization condition, Eq. (23), we find the Lagrange multiplier

$$\alpha = 8\pi I_2 a^3\sqrt{\tau - \lambda}/g_3^2. \tag{42}$$

Evaluating the functional $S[\eta]$ at $\eta = \eta_{drop}$ yields

$$S(\lambda) = \frac{2}{3g_3^2}\int d\mathbf{x}\,\eta_{drop}^3 = \frac{8\pi}{3g_3^2}a^3 I_3(\tau - \lambda)^{3/2}, \tag{43}$$

where integrals I_n are defined by

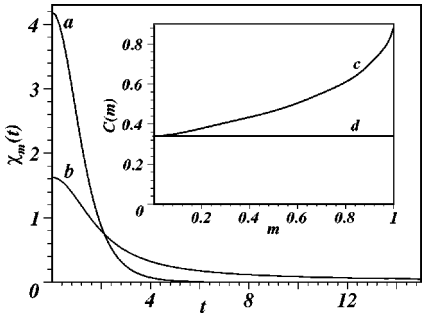

FIG. 2. Line a describes $\chi_0(t)=\chi(t)$ and line b gives $\chi_1(t)$. Line c in the inset shows the function $C(m)$ while line d corresponds to $C(0)=C$.

$$I_n=\int_0^\infty \chi_0^n(t)t^2dt. \tag{44}$$

Numerical integration yields

$$\chi(0)\simeq 4.19,\ I_2\simeq 1.73,\quad I_3\simeq 3.46,\quad \text{and}\quad I_4\simeq 8.82. \tag{45}$$

Steepest descent evaluation of the density of states Eq. (30), using the definition of the average Eq. (17), yields $g(\lambda)\propto\exp[-S(\lambda)]$. The calculation of the preexponential factor in this expression is nontrivial and requires the consideration of the excited states, with eigenvalues larger than the ground state, $\lambda_0<0$. Taking into account the contributions of the Goldstone modes (with $\lambda=0$) one obtains (Appendix A)

$$g(\lambda)\simeq \frac{D}{\tau-\lambda}\frac{S^2(\lambda)}{R^3(\lambda)}e^{-S(\lambda)}, \tag{46}$$

where D is a normalization constant.

We now return to the expression for the energy of a droplet, Eq. (25). Substituting the variational ground state solution $\psi_0(x)$, Eq. (36), we find

$$\frac{E^0_{drop}(\lambda)}{k_BT}=-\frac{6\pi a^3\lambda^2}{g_4(\tau-\lambda)^{3/2}}C,\quad C=\frac{I_2^2}{I_4}\simeq 0.34. \tag{47}$$

Since the true ground state energy is always lower than the variational estimate, the above procedure overestimates the energy $E_{drop}(\lambda)$. As shown in Appendix B, minimization of the exact energy functional, Eq. (20), yields an expression for the energy that can be written in the form of Eq. (47), provided that we replace the constant C by the function $C(m)$ of the parameter $m=-\lambda/(\tau-\lambda)$. A plot of $C(m)$ vs m is shown as curve c in the inset of Fig. 2.

The horizontal line d in this inset shows the value of $C=C(0)$ obtained by the variational approach, Eq. (47). In agreement with the inequality $E_{drop}(\lambda)\leqq E^0_{drop}(\lambda)$, the curve $C(m)$ always lies above this line and coincides with it at $m=0$ ($\lambda=0$). In the opposite limit, $m=1$ ($|\lambda|\gg\tau$, in the vicinity of the spinodal), the function $\psi(r)$ is calculated numerically [see Eq. (B1) of Appendix B and curve b in Fig. 2].

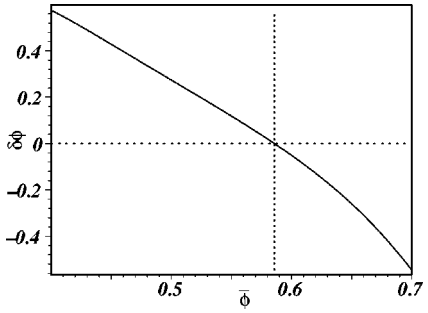

FIG. 3. Amplitude of droplet as a function of mean volume fraction, for $\theta=0.5$ and $\tau=0$.

The free energy is calculated by steepest descent estimate of the integral, Eq. (29). In this approximation, the free energy of the droplet is $\Delta F_{drop}(\lambda^*)=E_{drop}(\lambda^*)+k_BTS(\lambda^*)$ where λ^* minimizes the expression

$$\frac{\Delta F_{drop}(\lambda)}{k_BT}=-6\pi C\left(\frac{-\lambda}{\tau-\lambda}\right)\frac{\lambda^2a^3}{(\tau-\lambda)^{3/2}g_4}+\frac{8\pi}{3g_3^2}a^3I_3(\tau-\lambda)^{3/2}. \tag{48}$$

Since a minimum exists only for

$$\tau<\tau_D\simeq 0.145\frac{g_3^2}{g_4}, \tag{49}$$

τ_D can be interpreted as the stability limit of the droplet phase.

Our steepest descent evaluation of Eq. (29) is valid for $|\Delta F_{drop}(\lambda^*)|\gg k_BT$. Since g_3, $g_4\sim 1/N$, we have $|\Delta F_{drop}(\lambda^*)|/k_BT\sim\sqrt{N}$ and this condition is nearly always satisfied for sufficiently high degrees of polymerization (except in the immediate vicinity of the critical point). The presence of a deep minimum of the free energy suggests that long-lived droplets with composition $\phi\simeq\bar{\phi}+2a^{3/2}\sqrt{\bar{\phi}(1-\bar{\phi})}\psi_0$ appear following a quench to $\tau<\tau_D$. Notice that such long-lived droplets are quite different from critical droplets that lead to the decay of the homogeneous metastable phase when the system is quenched inside the binodal (between the binodal and the spinodal) in classical theories of nucleation and growth [4]. These critical nuclei are unstable, have an interface that is much thinner than their radius, and their bulk composition coincides with that of the final equilibrium phase [12]. In contrast, our droplets are locally stable, with an interface that is of the order of the size of the droplet, and concentration at their center that deviates by an amount

$$|\delta\phi(0)|=2a^{3/2}\sqrt{\bar{\phi}(1-\bar{\phi})}|\psi(0)|=\frac{|\lambda^*|}{g_3}a^{3/2}\sqrt{\bar{\phi}(1-\bar{\phi})}\chi_0(0)\ll 1, \tag{50}$$

from the mean $\bar{\phi}$ (see Fig. 3). Consequently the droplet so-

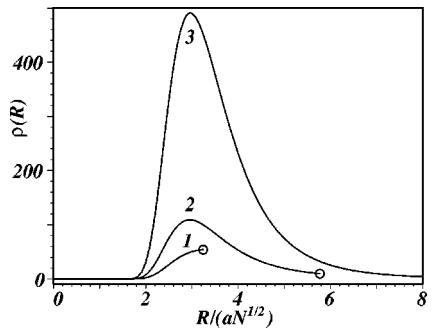

FIG. 4. Distribution function of the droplet radii for $\tau=\tau_D$ (curve 1), $0<\tau<\tau_D$ (curve 2), and $\tau=0$ (curve 3). The value of $R_{\max}$ for each of the curves is shown by a circle.

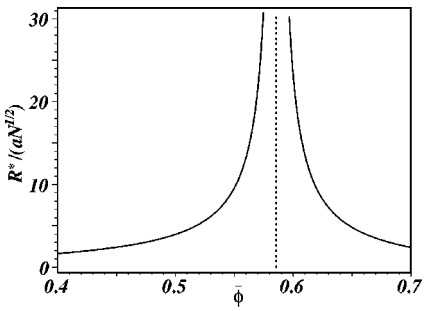

FIG. 5. Radius of droplet as a function of mean volume fraction, for $\theta=0.5$ and $\tau=0$.

lution for ψ satisfies the condition of applicability of the Landau expansion, Eq. (8).

In order to get further insight into the physical meaning of our droplet solution, we take note of the fact that the integrand in Eq. (29) can be interpreted as the Boltzmann weight of droplets corresponding to a given λ. The one-to-one relation between the eigenvalue λ and the radius of the droplet R, Eq. (41), allows us to write the Boltzmann weight of droplets with sizes in the interval $(R,R+dR)$ in the form $\rho(R)(V/R^3)dR/R$, where V is the volume of the system and the dimensionless distribution function of droplets of size R is defined by

$$\rho(R)=2DS^2[\lambda(R)]\exp\left\{-S[\lambda(R)]-\frac{E_{drop}[\lambda(R)]}{k_BT}\right\}. \tag{51}$$

In the range $0<\tau<\tau_D$ this distribution is sharply peaked about $R^*=R(\lambda^*)$, with R extending up to a cutoff $R_{\max}$ that corresponds to the maximal value of $|\lambda|$ for which a droplet solution exists, $\lambda_c=0$ (see Fig. 4). Since the amplitude of the ground state solution c_0 vanishes in the limit $\lambda_c=0$, the ground state dominance approximation that leads to Eq. (27) breaks down. At $\tau=\tau_D$ the values of R^* and $R_{\max}$ coincide and above τ_D the distribution is monotonically increasing with R. $R_{\max}$ increases monotonically with τ and diverges as $\tau\to 0$.

Notice that once a droplet of radius R^* is formed, it can only decay if, in the process of thermal fluctuations, it reaches the critical size $R_{\max}$. Since the decay time is proportional to the ratio $\rho(R^*)/\rho(R_{\max})$, inspection of Fig. 4 shows that it increases dramatically as the spinodal is approached.

Away from the critical point, the characteristic dimension of a droplet is of order $a\sqrt{N}$ and it diverges as $|\bar{\phi}-\bar{\phi}_c|^{-1}$ as the critical composition is approached (see Fig. 5).

IV. LATTICE OF DROPLETS

The many-droplet problem is prohibitively difficult and its exact solution is beyond the scope of this work (for an attempt to study the global equilibrium problem, see Ref. [13]). In the following, we will assume that the general solution $\psi(\mathbf{x})$ can be written as a superposition of many single-droplet contributions, Eq. (B1), with parameters treated as variational coefficients that minimize the free energy of the interacting many-droplet system. In order to understand how droplets will be distributed in space, one has to determine their interaction. Consider two droplets and assume for simplicity that both have the most probable size R^* corresponding to ground state eigenvalue λ^*. The droplets are centered about points $\mathbf{x}_1$ and $\mathbf{x}_2$, respectively, such that the distance between them $|\mathbf{x}_1-\mathbf{x}_2|$ is large with respect to $2R^*$. The field $\psi(\mathbf{x})$ that describes this configuration can be written as

$$\psi(\mathbf{x})=\psi_{drop}(\mathbf{x}-\mathbf{x}_1)+\psi_{drop}(\mathbf{x}-\mathbf{x}_2). \tag{52}$$

Substituting this expression into Eq. (20), we find the energy of the two-droplet configuration,

$$E=2E_{drop}+E_{int}(\mathbf{x}_1-\mathbf{x}_2), \tag{53}$$

where the main contribution to the interaction energy for well-separated droplets [the contributions that contain linear terms in $\psi_{drop}(\mathbf{x}_1-\mathbf{x})$ or $\psi_{drop}(\mathbf{x}_2-\mathbf{x})$ vanish because these functions minimize the energy functional, Eq. (20)] is

$$E_{int}(\mathbf{x}_1-\mathbf{x}_2)=\frac{g_4}{4}\int d\mathbf{x}\psi^2_{drop}(\mathbf{x}_1-\mathbf{x})\psi^2_{drop}(\mathbf{x}_2-\mathbf{x}). \tag{54}$$

When the distance between neighboring droplets, $|\mathbf{x}_1-\mathbf{x}_2|$, is large with respect to their characteristic size $R^*=a/\sqrt{\tau-\lambda^*}$, we can use the asymptotic form of the function $\psi_{drop}(\mathbf{x})$, Eqs. (B1) and (B5). Calculating the integral in Eq. (54) we find

$$E_{int}(\mathbf{x}_1-\mathbf{x}_2)=\frac{9(\lambda^*)^2a^3}{g_4(\tau-\lambda^*)^2}\frac{\pi^3a}{|\mathbf{x}_1-\mathbf{x}_2|}\exp\left(-\frac{2\sqrt{\tau}|\mathbf{x}_1-\mathbf{x}_2|}{a}\right). \tag{55}$$

Since the above expression is positive definite we conclude that droplets always repel each other and that the Coulomb-like $|\mathbf{x}_1-\mathbf{x}_2|^{-1}$ interaction is screened on a distance of order of the correlation length $\xi=a/\sqrt{\tau}$, Eq. (B6).

When the blend is quenched into the region $\tau<\tau_D$ (indicated by the arrow in Fig. 1) in which the free energy well corresponding to an isolated droplet is much deeper than k_BT, we expect that droplets will appear spontaneously in the entire volume of the sample. This process will continue until

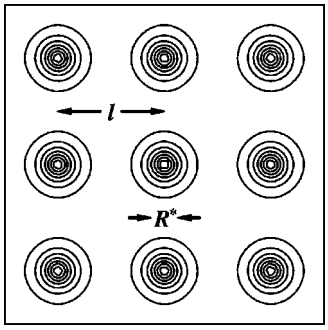

FIG. 6. Schematic contour plot of a two-dimensional cut through the lattice of droplets, in the vicinity of the spinodal (the coutours describe lines of equal volume fraction ϕ).

the free energy reduction due to droplet formation is balanced by interdroplet repulsion. The presence of strong (the interaction between the droplets at separations of the order of their dimensions is much larger than k_BT) long range Coulomb-like repulsion resembles the interaction between highly charged colloids and raises the possibility that the droplets form a Wigner crystal with lattice spacing much larger than their size. The analogy is incomplete since in our case both the number of droplets and their shape can be adjusted in order to reduce the repulsion and minimize the free energy. In the following, we shall not consider the delicate questions of long range order and symmetry of the droplet lattice, and will characterize it by an effective coordination number z and a characteristic distance l between neighboring droplets (see Fig. 6).

In order to account for effect of interdroplet repulsions on the shape of individual droplets, we use Feynman's variational principle $\Delta F \leqslant \Delta F_{var}$, where ΔF and ΔF_{var} are the true and the variational free energies of the droplet lattice, respectively. The latter is calculated using a trial field $\psi_{var}(\mathbf{x})$, chosen as a superposition of many single droplet contributions, Eq. (B1), with coordinates of the center of mass $\{\mathbf{x}_i\}$ corresponding to K lattice points,

$$\psi_{var}(\mathbf{x}) = \sum_{i=1}^{K} \psi_{drop}(\mathbf{x}-\mathbf{x}_i). \tag{56}$$

The function $\psi_{drop}(\mathbf{x})$ is determined by Eq. (56) in which the experimentally measurable parameter τ is replaced by a variational parameter τ_{var}. Substituting Eq. (56) into the effective Hamiltonian, Eq. (20), we find the energy of a lattice of droplets,

$$H_\eta[\psi_{var}] = K\left[E_{drop} + (\tau-\tau_{var})\frac{\partial E_{drop}}{\partial \tau_{var}}\right] + \sum_{i\neq j} E_{int}(\mathbf{x}_i-\mathbf{x}_j), \tag{57}$$

where E_{drop} is the energy of single droplet configuration given in Eq. (B8), with the substitution $\tau \to \tau_{var}$. The values of l and τ_{var} are found from the condition that they minimize the variational lattice free energy

$$\Delta F_{var} = H_\eta[\psi_{var}] + k_BTKS(\lambda). \tag{58}$$

Since the droplet phase disappears at $\tau \simeq \tau_D$, we will consider sufficiently deep quenches to the vicinity of the spinodal, for which $\tau \ll \tau_D$. Assuming that $\tau_{var} \ll |\lambda|$ we find that λ coincides with the ground state eigenvalue λ^* of the single droplet solution. Minimizing Eq. (58) with respect to τ_{var} and l we get

$$\tau_{var} \simeq \frac{C^2(1)}{4}|\lambda^*| \simeq 0.19|\lambda^*|, \quad l = \frac{a}{2\sqrt{\tau_{var}}}\ln(3z\pi^2). \tag{59}$$

This confirms the self-consistency of the assumptions $l \gg R^* \simeq a|\lambda^*|^{-1/2}$ and $\tau_{var} \ll |\lambda^*|$ used in the derivation of Eq. (59).

V. DISCUSSION

Our analysis shows that a new type of metastable state can form when a homogeneous polymer blend undergoes an off-critical quench to the vicinity of the mean field spinodal. This state consists of spherical droplets each of which corresponds to a deep local minimum (of order $\sqrt{N}k_BT$) of the free energy, compared to the initial homogeneous phase. The radius of the droplets diverges and the deviation from the mean concentration vanishes with the approach to the critical point. Away from the critical point, a finite concentration contrast between the droplet and the background develops, and its radius decreases and approaches polymer dimensions. We find that the interaction between droplets is purely repulsive, of a screened Coulomb type, and conclude that close to the spinodal such droplets will form spontaneously everywhere inside the volume of the blend. Although detailed considerations regarding the possibility of long range order in the resulting droplet ''lattice'' are beyond the scope of this work, the analogy with Wigner crystals suggests the presence of at least short range liquidlike order. Even though the lattice of droplets has a higher free energy than that of the two coexisting homogeneous phases of different polymer concentrations, the height of the free energy barrier for the dissolution of a droplet diverges as $\sqrt{N}k_BT$ in the limit of high molecular weight, suggesting that the droplet phase may be practically stable on experimentally accessible time scales. Apart from its fundamental importance, the existence of such a long-lived droplet phase may have interesting practical applications in polymer composites technology since it implies that one can, by an appropriate choice of parameters, limit the segregation of the components of the blend to length scales in the range of hundreds of angstroms while keeping the mixture of two high molecular weight polymers macroscopically homogeneous.

A schematic phase diagram of a polymer blend based on the above considerations is presented in Fig. 7. Notice that even though droplet solutions have no peculiarities at the spinodal, strictly speaking, our thermodynamic considerations break down somewhere beyond the limit of stability of the homogeneous phase, and one must go beyond the Landau expansion, Eq. (8), and consider the complete nonlinear problem.

We would like to stress that even though our prediction of

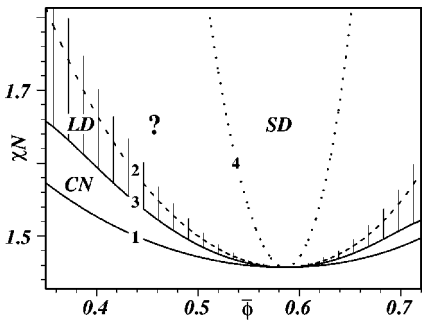

FIG. 7. Schematic phase diagram. In the CN region between lines 1 (binodal) and 3, the initial homogeneous phase decays through the formation of critical nuclei. The LD region corresponds to the metastable lattice of droplets and extends from line 3 to somewhere above the broken line 2 (spinodal). Spinodal decomposition (SD) takes place in the region limited by line 4. The domain between the LD and SD regions (question mark) is outside the scope of the present work.

a metastable droplet lattice appears to be supported by light scattering and microscopy observations of arrested droplet growth in Refs. [2] and [3], these experiments report observations of domains of size exceeding $10\mu m$ that form during the late stages of phase separation, and are unrelated to our droplets whose sizes and separations are smaller by three orders of magnitude (of the order of polymer size). The latter can be observed by neutron and x-ray scattering on polymer blends in which one of the polymeric components is labeled. To the best of our knowledge, the only published neutron scattering study of off-critical quenches into metastable and unstable regions of the phase diagram was done on a ternary blend of two model polyolefins (one of the components was deuterated) and a copolymer [14], to which our theory is not directly applicable. Although several peaks with amplitude decreasing with increasing wave vectors were observed by small-angle neutron scattering (SANS) for quenches into the metastable region [see Fig. 1(b) in Ref. [14]], the corresponding wavelengths were an order of magnitude larger than polymer dimensions. In a recent unpublished SANS study on a binary blend, a peak in the scattering developed rapidly following a pressure quench to the vicinity of the spinodal [15] (no scattering peaks were observed for quenches into the metastable region outside the spinodal). While the reported observation that the length scale of the ''nucleating entities'' does not increase with the approach to the spinodal, is inconsistent with classical theories of nucleation and spinodal decomposition, it agrees with our predictions. However, since the smallest length scale reported in this SANS study (400 Å) exceeds the radii of gyration of the polymers (160 Å), a detailed comparison with our theory requires extending the experiment to larger scattering wave vectors or increasing the molecular weight of the components of the mixture. The latter alternative has the advantage that since the Ginzburg number decreases with increasing N, the validity of our mean field approximations improves with increasing degree of polymerization. Working with very high molecular weights may in fact be necessary for observing the predicted behavior, since numerical simulations suggest that the Ginzburg number in blends is unexpectedly large for values of N commonly used in experiments [16].

A possible criticism of our analysis is that the de Gennes–Flory–Huggins free energy, Eq. (1), does not provide a satisfactory description of the blend on length scales of the order of polymer dimensions and that a more refined theory (see, e.g., Refs. [17] and [18]) is needed. While this is strictly true, the derivation of the droplet solution is based only on the GL Hamiltonian, Eq. (8), which is the generic phenomenological functional for the description of first order phase transitions. The only polymer-specific characteristic is the small magnitude of the Ginzburg number or, equivalently, the anomalously small amplitude of thermal fluctuations in the vicinity of the spinodal. This guarantees the validity of mean field arguments that allow the replacement of the term cubic in ψ in the original GL Hamiltonian by a random field that acts as an attractive potential that leads to the appearance of localized droplet solutions. We would like to caution that while the derivation of the single droplet solution is robust, the validity of the tentative analysis of the lattice of droplets in Sec. IV is open to question and further analytical and numerical studies of this collective state are clearly necessary. If our conjectures concerning the lattice of droplets are correct, metastable droplet phases in the vicinity of the spinodal are expected in other physical systems described by the Hamiltonian Eq. (8) and characterized by a small Ginzburg number, such as ^{3}He–^{4}He mixtures [19], and magnetic materials in which there are competing antiferromagnetic and ferromagnetic interactions [20].

ACKNOWLEDGMENTS

Helpful discussions with B. Shapiro and S. Reich and written correspondence with N. Balsara and T. Hashimoto are gratefully acknowledged. Y.R. would like to acknowledge the support by a grant from the Israel Science Foundation.

APPENDIX A: GOLDSTONE MODES OF THE DROPLET

In order to utilize standard methods of theoretical solid state physics developed in the context of electron localization in a random field, we first derive a field-theoretical representation for the density of states $g(\lambda)=\langle\delta[\lambda-\lambda_0(\eta)]\rangle_\eta$, Eq. (30).

We begin with the equality

$$\delta[\lambda-\lambda_0(\eta)]=-\frac{1}{\pi}\mathrm{Im}\frac{1}{\lambda-\lambda_0(\eta)+i0}, \tag{A1}$$

where $i0$ denotes $\lim i\varepsilon$ as ε approaches zero from above, and represent the two-point correlator of the field $\psi(\mathbf{x})$ as

$$\langle\psi(\mathbf{x}_1)\psi(\mathbf{x}_2)\rangle=\sum_k\frac{\psi_k(\mathbf{x}_1)\psi_k(\mathbf{x}_2)}{\lambda-\lambda_k(\eta)+i0}. \tag{A2}$$

The average in the above expression is taken with the weight $\exp(-H_\eta^{(2)}[\psi]/k_BT)$, where the quadratic contribution to the Hamiltonian $H_\eta[\psi]$, Eq. (20), is given by

$$\frac{H_\eta^{(2)}[\psi]}{k_BT}=\int d\mathbf{x}\left[\frac{\tau-\eta-\lambda-i0}{2}\psi^2+\frac{a^2}{2}(\nabla\psi)^2\right]. \quad \text{(A3)}$$

Since we are interested in a situation when the ground state dominance approximation is valid, we only keep the $k=0$ contribution in Eq. (A2). Taking into account the normalization condition, Eq. (23), we find from Eqs. (A1) and (A2),

$$\delta[\lambda-\lambda_0(\eta)]\simeq-\frac{1}{\pi}\int d\mathbf{x}\,\mathrm{Im}\,G_0(\mathbf{x},\mathbf{x}), \quad \text{(A4)}$$

$$G_0(\mathbf{x}_1,\mathbf{x}_2)=\lim_{n\to0}\int D\vec{\psi}\psi^1(\mathbf{x}_1)\psi^1(\mathbf{x}_2)e^{-H_\eta^{(2)}[\vec{\psi}]},$$

where integration goes over n-component field $\vec{\psi}=\{\psi^1,\ldots,\psi^n\}$. Substituting this expression into Eq. (30) and integrating over the auxiliary field $\eta(\mathbf{x})$, using Eq. (17), we find

$$g(\lambda)=-\frac{1}{\pi}\int d\mathbf{x}\,\mathrm{Im}\,G(\mathbf{x},\mathbf{x}), \quad \text{(A5)}$$

$$G(\mathbf{x},\mathbf{x})=\lim_{n\to0}\int D\vec{\psi}\psi^1(\mathbf{x})\psi^1(\mathbf{x}')e^{-H^{(3)}[\vec{\psi}]}, \quad \text{(A6)}$$

where the effective Hamiltonian (up to cubic order in ψ) is given by

$$H^{(3)}[\vec{\psi}]=\int d\mathbf{x}\left[\frac{\tau-\lambda-i0}{2}\vec{\psi}^2+\frac{a^2}{2}(\nabla\vec{\psi})^2-\frac{g_3}{6}(\vec{\psi}^2)^{3/2}\right]. \quad \text{(A7)}$$

Even though we are interested in the density of states associated with the minimal eigenvalue λ_0 of Eq. (22), our result, Eq. (A5), is more general and gives the contribution of all the excited modes of the droplet (deviations from spherical shape).

It is easy to check that the steepest descent evaluation of the integral, Eq. (A5), gives $g(\lambda)\simeq e^{-S(\lambda)}$ where $S(\lambda)=\min_\psi H^{(3)}[\vec{\psi}]$ is given in Eq. (43) and that $H^{(3)}[\vec{\psi}]$ is minimized by the instanton configuration of the field $\vec{\psi}$,

$$\vec{\psi}_{inst}(\mathbf{x})=\psi_{inst}(r)\vec{e},\quad \psi_{inst}(r)=\frac{\tau-\lambda}{g_3}\chi_0\left(\frac{r\sqrt{\tau-\lambda}}{a}\right). \quad \text{(A8)}$$

Here $\vec{e}$ is an arbitrary unit vector in n-dimensional "isotopic" space.

In order to calculate the preexponential factor we need to take into account contributions from excited states, with eigenvalues larger than λ_0. We expand the effective Hamiltonian about the instanton configuration, $\delta\vec{\psi}(\mathbf{x})=\vec{\psi}(\mathbf{x})-\vec{\psi}_{inst}(r)$ [21],

$$\delta H^{(3)}[\vec{\psi}]=\frac{1}{2}\int d\mathbf{x}\sum_{ij}\delta\psi_i M_{ij}\delta\psi_j. \quad \text{(A9)}$$

The operator $\mathbf{M}$ of this quadratic form can be decomposed into transverse and longitudinal parts,

$$M_{ij}=M^L e_i e_j+M^T(\delta_{ij}-e_i e_j), \quad \text{(A10)}$$

$$M^L=\tau-\lambda-a^2\nabla^2-g_3\psi_{inst}(r),$$

$$M^T=\tau-\lambda-a^2\nabla^2-\frac{1}{2}g_3\psi_{inst}(r).$$

Introducing the orthonormal set of eigenfunctions of the operators M_L and M_T

$$M^L\psi_k^L=\lambda_k^L\psi_k^L,\quad M^T\psi_k^T=\lambda_k^T\psi_k^T, \quad \text{(A11)}$$

we expand $\delta\vec{\psi}(\mathbf{x})$ over these normal modes,

$$\delta\vec{\psi}(\mathbf{x})=\psi^L(\mathbf{x})\vec{e}+\vec{\psi}^T(\mathbf{x}), \quad \text{(A12)}$$

$$\psi^L(\mathbf{x})=\sum_k c_k\psi_k^L(\mathbf{x}),\quad \vec{\psi}^T(\mathbf{x})=\sum_l\sum_k\vec{c}_k^{\,l}\psi_k^T(\mathbf{x}),$$

where the $n-1$ vectors $\vec{c}_k^{\,l}$ $(l=1,\ldots,n-1)$ for each k are orthogonal to each other and to the vector $\vec{e}$.

Consider first the Goldstone modes that correspond to eigenvalues $\lambda_k=0$. Our heuristic derivation below follows that of Ref. [22]. The variation of the field induced by the translation of an instanton in regular three-dimensional space by a distance $\delta\mathbf{x}_0$ is

$$\delta\vec{\psi}(\mathbf{x})=\vec{\psi}_{inst}(\mathbf{x}+\delta\mathbf{x}_0)-\vec{\psi}_{inst}(\mathbf{x})=\sum_i\frac{\partial\vec{\psi}_{inst}(\mathbf{x})}{\partial x_i}\delta x_{0i}. \quad \text{(A13)}$$

Imposing the standard normalization condition, $\int d\mathbf{x}\psi_k^2(\mathbf{x})=1$, yields

$$\psi_{1i}^L(\mathbf{x})=J_L^{-1/2}\frac{\partial\psi_{inst}(\mathbf{x})}{\partial\mathbf{x}},\quad J_L=\int d\mathbf{x}\left[\frac{\partial\psi_{inst}(r)}{\partial x_i}\right]^2. \quad \text{(A14)}$$

Comparing Eqs. (A12) and (A13), we find

$$dc_{1i}=J_L^{1/2}dx_{0i} \quad \text{(A15)}$$

for each one of three translational modes. Since the eigenvalue $\lambda_1^L=0$ of the Schrödinger equation, Eq. (A11) for $\psi_1^L(\mathbf{x})$ is degenerate (there are three eigenfunctions corresponding to this eigenvalue), we conclude that it does not correspond to the nondegenerate ground state and that the latter should have a negative eigenvalue, $\lambda_0^L<0$. In the language of atomic physics, translational Goldstone modes correspond to triply degenerate (dipolar) p states, while the ground state is a spherically symmetric s state.

Now consider rotational modes, which correspond to a rotation of unit vector $\vec{e}$ (in the n-dimensional "isotopic" space) by an arbitrary vector $\delta\vec{e}^{\,l}$, orthogonal to the vector $\vec{e}$,

$$\delta\vec{e}^{\,l}\cdot\vec{e}=0. \tag{A16}$$

This rotation is determined by the $n-1$ independent angles, $l=1,\ldots,n-1$. The variation of the field induced by an infinitesimal rotation, $\vec{e}\to\vec{e}+\delta\vec{e}^{\,l}$, is

$$\delta\vec{\psi}(\mathbf{x})=\sum_l \psi_{inst}(r)\,\delta\vec{e}^{\,l}=\sum_l J_T^{1/2}\psi_0^T(\mathbf{x})\,\delta\vec{e}^{\,l}, \tag{A17}$$

where the rotational eigenfunction is

$$\psi_0^T(\mathbf{x})=J_T^{-1/2}\psi_{inst}(\mathbf{x}),\quad J_T=\int d\mathbf{x}\psi_{inst}^2(r). \tag{A18}$$

Comparing Eqs. (A12) and (A17), we find

$$d\vec{c}_0^{\,l}=J_T^{1/2}\delta\vec{e}^{\,l} \tag{A19}$$

for each one of $n-1$ rotational modes, which correspond to $n-1$ independent angles that characterize the orientation of the vector $\vec{e}$.

Calculating the Gaussian integrals over all c_k in Eq. (A6), we find the instanton contribution to the function $G(\mathbf{x}_1,\mathbf{x}_2)$,

$$G(\mathbf{x}_1,\mathbf{x}_2)=\lim_{n\to0}e^{-S(\lambda)}J_L^{3/2}J_T^{(n-1)/2}\prod_{k\neq1}\left(\frac{\pi}{\lambda_k^L}\right)^{1/2}\prod_{k\neq0}\left(\frac{\pi}{\lambda_k^T}\right)^{(n-1)/2}\times\int d\mathbf{x}_0\int d\vec{e}\,\psi_{inst}(\mathbf{x}_1-\mathbf{x}_0)\psi_{inst}(\mathbf{x}_2-\mathbf{x}_0). \tag{A20}$$

Since $\lambda_0^L<0$, this contribution is imaginary. Using Eq. (A8) we can easily estimate the Jacobians,

$$J_L\simeq S(\lambda)/a^2,\quad J_T\simeq S(\lambda)/(\tau-\lambda). \tag{A21}$$

Expression (A20) can be further simplified by means of dimensionless analysis if we notice that λ_k^L and λ_k^T are both proportional to $\tau-\lambda$. Substituting Eq. (A20) into Eq. (A5) and taking the limit $n\to0$, we arrive at Eq. (46).

APPENDIX B: NUMERICAL MINIMIZATION OF THE ENERGY

In the following we carry out numerical minimization of the energy functional, Eq. (20). Since the ground state solution is spherically symmetric and therefore depends on the radial coordinate r only, it is convenient to express it through a dimensionless function $\chi_m(t)$ of the dimensionless length $t=r\sqrt{\tau-\lambda}/a$,

$$\psi_{drop}(r)=\sqrt{\frac{-6\lambda}{g_4}}\chi_m\left(\frac{r\sqrt{\tau-\lambda}}{a}\right). \tag{B1}$$

Minimizing the Hamiltonian, Eq. (20), with respect to $\psi(r)$ yields the equation

$$\chi_m''+2\chi_m'/t=(1-m-\chi)\chi_m+m\chi_m^3,\quad m=-\lambda/(\tau-\lambda), \tag{B2}$$

with boundary conditions

$$\chi_m'(0)=0,\quad \chi_m(t\to\infty)=0. \tag{B3}$$

Comparing Eqs. (B2) and (37) we conclude that $\chi_0(t)=\chi(t)$.

At small t the solution of Eq. (B2) can be expanded as

$$\chi_m(t)=\chi_m(0)\left[1-\frac{\chi(0)-1+m-m\chi_m^2(0)}{6}t^2+\cdots\right], \tag{B4}$$

while for $t\to\infty$ it decays as

$$\chi_m(t)\simeq t^{-1}e^{-\sqrt{1-m}t}. \tag{B5}$$

We conclude that in contrast to the variational solution, Eq. (21), the function $\psi_{drop}(r)$ has two characteristic scales,

$$R=a/\sqrt{\tau-\lambda}\quad\text{and}\quad\xi=a/\sqrt{\tau}. \tag{B6}$$

In general, for $\lambda<0$ we have $R<\xi$, and the two lengths coincide only in the case of a critical droplet, $\lambda=0$. According to our analysis, R determines the characteristic size of the potential well [see Eq. (41)], while ξ is the correlation radius of the system, which diverges at spinodal. Inspection of Eq. (B2) shows that it can be simplified in two limiting cases. For $\lambda=0$ (i.e., $m=0$) this equation reduces to Eq. (37) and its solution coincides with the variational one, $\chi_0(t)$ [curve a in Fig. 2]. In the limit of small $\tau(\ll|\lambda|)$ that corresponds to $m\to1$, numerical calculations show that the solution factorizes into a product of functions of R and of ξ,

$$\psi_{drop}(r)=\sqrt{\frac{-6\lambda}{g_4}}\chi_1\left(\frac{r}{R}\right)\left(1+\frac{r}{\xi}\right)e^{-r/\xi}, \tag{B7}$$

where the solution $\chi_1(t)$ of Eq. (B2) with $m=1$ decays as a power, $\chi_1(t)\sim t^{-1}$ as $t\to\infty$ (see curve b in Fig. 2).

Substituting the numerical solution for $\psi_{drop}(r)$ into Hamiltonian Eq. (20), we find

$$\frac{E_{drop}(\lambda)}{k_BT}=-\frac{6\pi a^3\lambda^2}{g_4(\tau-\lambda)^{3/2}}C\left(\frac{-\lambda}{\tau-\lambda}\right),\qquad C(m)=\int_0^\infty dt t^2\chi_m^4(t), \tag{B8}$$

which has the same form as that of the variational energy, Eq. (47), with $C=C(m=0)$ replaced by $C(m)$.

[1] P.-G. de Gennes, *Scaling Concepts in Polymer Physics* (Cornell, Ithaca, 1979).
[2] T. Hashimoto, M. Takenaka, and T. Izumitani, J. Chem. Phys. **97**, 679 (1992); M. Takenaka, T. Izumitani, and T. Hashimoto, *ibid.* **98**, 3528 (1993); H. Takeno and T. Hashimoto, *ibid.* **108**, 1225 (1998).
[3] D. Katzen and S. Reich, Europhys. Lett. **21**, 55 (1993).
[4] J.D. Gunton, M. San Miguel, and P.S. Sahni, in *Phase Transitions and Critical Phenomena* edited by C. Domb and J. Lebowitz (Academic, New York, 1983), Vol. 8, p. 269.
[5] M.A. Kotnis and M. Muthukumar, Macromolecules **25**, 1716 (1992).
[6] L. Sung, A. Karim, J.F. Douglas, and C.C. Han, Phys. Rev. Lett. **76**, 4368 (1996).
[7] P.-G. de Gennes, J. Phys. (France) Lett. **38L**, 441 (1977); J. Chem. Phys. **72**, 4756 (1980).
[8] P.J. Flory, *Principles of Polymer Chemistry* (Cornell, Ithaca, 1953).
[9] J.-F. Joanny, J. Phys. A **11**, L117 (1978); K. Binder, J. Chem. Phys. **79**, 6387 (1983).
[10] A.M. Polyakov, *Gauge Fields and Strings* (Harwood Academic, New York, 1987).
[11] L.B. Ioffe and A.I. Larkin, Zh. Éksp. Teor. Fiz. **81**, 707 (1981) [Sov. Phys. JETP **54**, 378 (1981)].
[12] A.Z. Patashinskii and B.I. Shumilo, Zh. Éksp. Teor. Fiz. **77**, 1417 (1979) [Sov. Phys. JETP **50**, 712 (1979)].
[13] V.S. Mitlin and L. Manevich, Vysokomol. Soedin., Ser. A **30**, 9 (1988).
[14] N.P. Balsara, C. Lin, and B. Hammouda, Phys. Rev. Lett. **77**, 3847 (1996).
[15] A.A. Lefebvre, J.H. Lee, N.P. Balsara, and B. Hammouda, J. Chem. Phys. **116**, 4777 (2002).
[16] K. Binder, H.-P. Deutsch, U. Micka, and M. Muller, Nucl. Phys. B Proc. Suppl. **42**, 27 (1995).
[17] E. Reister, M. Müller, and K. Binder, Phys. Rev. E **64**, 041804 (2001).
[18] S.M. Wood and Z.-G. Wang, J. Chem. Phys. **116**, 2289 (2002).
[19] M. Blume, V.J. Emery, and R.B. Griffiths, Phys. Rev. A **4**, 1071 (1971).
[20] D.R. Nelson and M.E. Fisher, Phys. Rev. B **11**, 1030 (1975).
[21] I.L. Cardy, J. Phys. C **11**, L321 (1978).
[22] C.G. Callan and S. Coleman, Phys. Rev. D **16**, 1762 (1977).